Cement & Concrete Composites 60 (2015) 99–110

Contents lists available at ScienceDirect

Cement & Concrete Composites

journal homepage: www.elsevier.com/locate/cemconcomp

Bentonite as a natural additive for lime and lime–metakaolin mortars used for restoration of adobe buildings

S. Andrejkovičová [a,*], C. Alves [b], A. Velosa [b], F. Rocha [a]

[a] Geosciences Department, Geobiotec Research Unit, University of Aveiro, Campus Universitário de Santiago, 3810-193 Aveiro, Portugal
[b] Civil Engineering Department, Geobiotec Research Unit, University of Aveiro, Campus Universitário de Santiago, 3810-193 Aveiro, Portugal

ARTICLE INFO

Article history:
Received 5 January 2015
Received in revised form 19 March 2015
Accepted 6 April 2015
Available online 16 April 2015

Keywords:
Lime
Bentonite
Metakaolin
Mortar
Mechanical properties
Artificial ageing
Adobe
Restoration

ABSTRACT

This work estimates the behaviour of mortars based on lime, seeking their application as renders of adobe walls. Mortars with binder:aggregate 1:3 volumetric ratio were prepared as is traditionally used in old buildings in central parts of Portugal.

Due to specificity of the support, two clays, natural clay bentonite (5 wt.%) and artificial clay metakaolin (20 wt.%) were used as additives to lime mortar to prepare 3 types of blended mortars, besides the air lime reference mortar. Mortar prisms 4 × 4 × 16 cm were analysed to assess mechanical properties and salt resistance. Moreover, the mortars were placed in three ways on old adobes taken from demolished houses and their behaviour was verified by artificial accelerated ageing test. Lastly, mortars were applied on a wall made from traditional adobes, where panels were monitored and trials with adhesion strength and Karsten tubes have been conducted. The results obtained by comparison of the characteristics from all the experimental procedures reveal that mortar containing air lime and 5 wt.% of bentonite fulfils in the best way the requirements in its use as render of adobe buildings.

1. Introduction

Depending on the local tradition, various types of earthen construction were used in the central parts of Portugal, up to the beginning of the 20th century. There is an evident presence of an important legacy of adobe construction in Portugal, with a special territorial focus on the area between Murtosa and Mira/Figueira da Foz, extending as well to inland areas [1]. Currently many edifices constructed from adobe bricks still persist, both in city centres and in rural areas. Moreover; many urban adobe buildings show a cultural, historical and architectonic recognized value, for example the ornate buildings with an "Art Nouveau" style [2]. Unfortunately, the degradation has affected many of these buildings and this is particularly evident in terms of the renders, because they are the exposed external element and extremely prone to the action of weather.

Rendering mortars play an important role in the conservation of earth based walls as their application has not only an aesthetical purpose, but also the protection and reduction of the wall's deterioration. They act as a "sacrifice" element and regulate water intake and output. Rendering mortars must also attain mechanical and chemical compatibility with adobe in order to promote its conservation [3–5]. Over the centuries, historic mortars have demonstrated to be long lasting and compatible with the historic structural units. Therefore, a design of new mortars should be approached by simulating the historic materials [3,6–8].

Lime has been used as a binder in architectural heritage mortars since prehistoric times and seems to be an extremely enduring binder. For this reason, air lime mortars and/or combined with pozzolans have been studied widely, with the objective to be used as mortars for the restoration of historic buildings (e.g. [6,9–14]). Addition of high reactive pozzolans to lime creates mortars similar to historic ones that exhibit improved values of mechanical strength and an advanced durability. Positive effect of metakaolin as a pozzolanic incorporation to mortars has been verified [15,16]. Moreover scientific attention is being focused also on utilization of natural clays and clay minerals due to their unique physico-chemical properties and/or optimal morphological structure as lime binder replacement. For instance sepiolite [17–20], palygorskite [21], zeolite [22,23], vermiculite [24] and bentonite [25–27] have been added to mortars and cements to improve their characteristics.

The last mentioned clay, bentonite (from Jelšový Potok (JP) deposit, Slovakia), was also used in the present work as an additive to air lime/metakaolin mortars due to its properties and the specificity of application on earth-based buildings.

* Corresponding author. Tel.: +351 234 370 747; fax: +351 234 370 605.
E-mail address: slavka@ua.pt (S. Andrejkovičová).

http://dx.doi.org/10.1016/j.cemconcomp.2015.04.005
0958-9465/

The quality of bentonitic raw materials depends on numerous parameters such as chemical stability, rheological and exchange properties, adsorption abilities and swelling behaviour. Bentonite (JP) due to its characteristics like high cation exchange capacity and specific surface area, has been recently studied predominantly in terms of environmental protection as sealing material in landfill liners [28,29], adsorbent of toxic heavy metals [30,31] and radionuclides in dependence on its use as a sealing barrier in radioactive waste and spent nuclear fuel repositories [32–37].

The main objective of this study is to create new repair mortars to be used as renders for historical adobe buildings, fulfilling compatibility requirements and showing improved mechanical and durability properties in comparison with reference air lime mortar. As coastal parts of the Iberian Peninsula, in which Portugal is included, are typical for harsh winds [38–40] combined in the summer by lack of humidity, mortar mixtures based on lime and/or metakaolin and bentonite were prepared. The main reason of choosing bentonite as an additive is that it is a natural pozzolan [26,27], economically friendly, has a high adsorption capacity with ability to retain water, hence able to support pozzolanic activity of metakaolin in case of low humidity conditions.

2. Materials used for mortars preparation

The materials used for preparation of mortars were the following: commercial air lime (AL) (Lusical H100, Portugal) with classification CL90, commercial metakaolin 1200S (MK) (AGS Mineraux, France), commercial bentonite (B) (type A 020, non-activated, natural, content of montmorillonite 65–85 wt.%, from Jelšový Potok (JP) deposit, Envigeo a.s., Banská Bystrica, Slovakia) and commercial sand (mixture of 3 sands APAS 12, APAS 20 and APAS 30 with volumetric ratios 1:1.5:1.5, respectively; Areipor – Areias Portuguesas, Lda, Bucelas, Portugal). Bulk densities of materials are reported in Table 1.

Four types of mortars were prepared with binder: sand – 1:3 volumetric ratio.

The first type of mortar (AL) used as reference contained air lime:sand in a 1:3 volumetric ratio. Blended mortars were prepared as follows:

(a) 5 wt.% of air lime was replaced by bentonite (BAL).
(b) 20 wt.% of air lime was replaced by metakaolin (AL20MK).
(c) Air lime was substituted by 5 wt.% of bentonite and 20 wt.% of metakaolin (BAL20MK). To achieve required consistency and appropriate workability (similar flow table values of around 120–130 mm), 20 wt.% of water was added to mortars [41].

Table 1
Bulk densities of materials (kg m^{-3}).

Material	Bulk density (kg m^{-3})
APAS 12	1444.4
APAS 20	1405.0
APAS 30	1381.3
Air lime	395.7
Metakaolin	296.0
Bentonite	719.3

All types of mortars were studied and analysed (a) as prisms, (b) applied on adobes, (c) applied on adobe walls according to Andrejkovičová et al. [18].

(a) Mortar testing as prisms

Mortar specimens 4 × 4 × 16 cm were prepared and cured as follows: air lime mortar without any additives was stored during all curing periods in a chamber with a relative humidity of 65 ± 5% and 20 ± 2 °C; while mortars containing metakaolin and bentonite were placed in moulds for the first 7 days at 20 ± 2 °C with a relative humidity of 95 ± 5% and then kept for 21 days in a chamber with relative humidity of 65 ± 5% and 20 ± 2 °C according to the Standard [42]. After removing the mortars from moulds, all the probes were stored at a chamber with relative humidity of 65 ± 5% and cured up to 28, 90 and 180 days.

(b) Mortars applied on adobes

Every mortar type was applied on adobes in three ways, simulating traditional application practices, as is shown in Fig. 1: (a) one layer of 2 cm (Adobe 1), (b) two layers; each layer with 2 cm, in total 4 cm (Adobe 2), (c) one mortar layer of 2 cm under which supporting spatterdash was used (Adobe 3). In case of adobes 2 and 3, a second mortar layer was applied 1 day after, when the bottom layer had dried.

(c) Mortars applied on adobe wall

Mortars were applied on the adobe wall in the most traditional way, similarly as is illustrated in Fig. 1 – adobe 3, to control if spatterdash fulfils a function of enhanced adhesion of mortar to support. Spatterdash layer was applied under 2 cm layer of individual mortar. This mortar layer was applied the day after, when the bottom layer had dried. Mortars were applied on adobe wall as squares with dimensions of 50 × 50 cm (Fig. 2). Mortars were cured in laboratory conditions and analysed after 30, 60 and 90 days.

3. Methods

Following techniques were used for:

3.1. Materials and/or mortar prisms

Philips X'Pert diffractometer equipped with Cu Kα radiation was used to establish mineralogical composition of the specimens. The X'Pert HighScore (PW3209) program was used to analyze XRD peaks.

Fig. 1. Application of mortars on adobes.

Fig. 2. Application of mortars on adobe wall.

The chemical composition (major elements) of materials was analysed using Panalytical Axios X-ray fluorescence spectrometer. Loss on ignition was determined by heating the samples in an electrical furnace at 1000 °C during 3 h.

The microstructural and chemical homogeneity was analysed by scanning electronic microscopy, SEM/EDS (Hitachi SU 70 coupled with EDAX Bruker AXS detector).

Carbonation degree was determined by a phenolphthalein solution (1%) and based on ICCROM's ARC test description [43].

Mechanical (flexural and compressive) strength tests were carried out on 3 probes of individual mortar on (SHIMADZU: AG-IC 100 kN) equipment, with loads of 10 and 50 kN/s for flexural and compressive strength, respectively; according to the Standard [42].

Test of mortars resistance to salts was performed by submerging (in the same way like in the Standard: Water absorption by capillary action [44]) the mortars for 7 h to NaCl solution (27 g NaCl in 1 L of water) in a climatic chamber at 20 °C and 65% of relative humidity. Then they were subjected for 17 h of drying in an oven at 65 °C. This procedure was repeated 10 times. At the end of each individual cycle, the specimens were weighed and visually examined to monitor any changes in their structure due to the deposition of salts. After 10 cycles, the samples were placed in a climatic chamber at 20 °C and 65% relative humidity for two weeks. At the end of this period, mortars were tested to verify their flexural and compressive strength and analysed by X-ray diffraction and scanning electron microscope (SEM-EDS).

3.2. Mortars applied on adobes

To study the effect of ageing of the mortars, they were subjected to accelerated weathering by simulating the atmospheric conditions (temperature and relative humidity) which occur during 1 year in the city of Aveiro (Portugal). Atmospheric conditions were set as extreme in order to incorporate all possible temperature variations in the district.

Mortars applied on adobes were subjected to 84 cycles of "summer/winter" in a climatic chamber (ESPEC: ARL-680) to analyse structural changes of mortars. Before exposure to artificial ageing, mortars were cured during a period of 1 month. Adobes containing AL were cured in a chamber with a relative humidity of 65 ± 5% and 20 ± 2 °C. Mortars with metakaolin and bentonite stayed for the first 7 days at 20 ± 2 °C with a relative humidity of 95 ± 5%, and then for 23 days in chamber at the same temperature but at with a relative humidity of 65 ± 5%.

Table 2
Climatic conditions subjected to adobes.

Primary cycle	Secondary cycle	Temperature (°C)	Relative humidity (%)
Summer (24 h)	Day (3 h)	60	95
	Night (3 h)	10	40
Winter (24 h)	Day (3 h)	30	95
	Night (3 h)	−10	95

The cycles were divided into primary "summer" and "winter" and secondary "day" and "night" cycles (Table 2). The first phase started with "summer-day" period (with temperature 60 °C and relative humidity 95%) and continued by "summer-night" (with temperature 10 °C and relative humidity 40%). Each secondary cycle had a duration of 3 h and was repeated 4 times, in order to achieve 24 h – the duration of the primary cycle.

After the "summer" cycle followed 24 h of "winter" cycle. Throughout this period, are also the secondary cycles ("day" with temperature 30 °C and relative humidity 95% and "night" with temperature −10 °C and relative humidity 95%). Summer and winter cycles were repeated 84 times, 42 times each. All adobes with individual mortars were weighed before testing and then after every week during subjection to artificial ageing.

3.3. Mortars applied on adobe wall

Adhesion of mortars on the supporting wall was determined according to the Standard EN 1015-12 [45]. On each type of mortar, two tests were carried out.

Karsten tube penetration test was used to measure water absorption by mortars. The Karsten tube was filled by water up to 4 ml. Time of water absorbed was measured after each ml [46,47]. Average value of 2 tests is reported.

4. Results and discussion

4.1. Mineralogical and chemical analysis of materials

4.1.1. X-ray diffraction (XRD) and X-ray fluorescence analysis (XRF) analyses

Mineralogical and chemical analyses of materials are presented in Fig. 3 and Table 3, respectively. All types of sand show alike XRD patterns composed of dominant mineral quartz with admixture of feldspar, what is in accordance with increased SiO_2, Al_2O_3 and K_2O in their chemical analyses. In the case of air lime, high percentage of calcium oxide (76.74%) is related to the presence of portlandite and calcite peaks (Fig. 3). Metakaolin sample contains diffractions of illite and quartz, and elevated value of TiO_2 (1.55%) in chemical analysis is associated with presence of anatase (Fig. 3 and Table 3). The main component of bentonite diffractogram is montmorillonite, in more detail according to chemical analysis Ca–Mg one, containing minor impurities of quartz, mica and feldspar (Fig. 3).

4.2. Testing of mortars as prisms

4.2.1. Mineralogical composition and degree of carbonation of non-treated mortars

Changes in mineralogical composition of mortars during curing at 28, 90 and 180 days were detected by XRD analysis (Fig. 4A–C). At 28 days, mortars without metakaolin AL and BAL are characterized by intense diffractions of portlandite, slightly more intense in

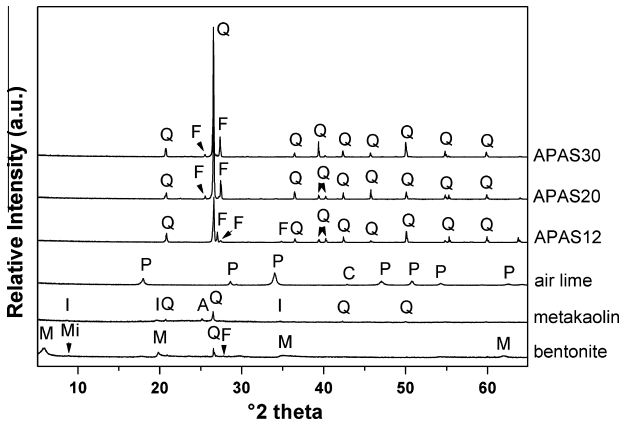

Fig. 3. X-ray diffraction patterns of random oriented materials. (A – anatase, C – calcite, F – feldspar, I – illite, M – montmorillonite, Mi – mica, P – portlandite, Q – quartz).

case of BAL (Fig. 4A). This is in accordance with the phenolphthalein test (Table 4), which shows that BAL mortar carbonates (23%) more slow as desired. On the other hand, in XRD patterns of AL20MK and BAL20MK dominate peaks of calcite and new diffraction peaks appear as a product of pozzolanic reaction between MK and portlandite attributed to monocarboaluminate $C_4A\bar{C}H_{11}$ ($3CaO{\cdot}Al_2O_3{\cdot}CaCO_3{\cdot}11H_2O$) at 11.6 and 23.4 °2$\theta$ (Fig. 4A).

At 90 days (Fig. 4B), calcite peaks dominate in all the mortars, however AL and BAL maintain a similar trend as at 28 days with quite intense portlandite diffractions. Again, BAL mortar displays the slowest carbonation (80%) (Table 4). Carbonation process is complete for BAL20MK, while AL20MK contains a minor amount of non-reacted portlandite (Fig. 3B, Table 4). In addition, diffractions of $C_4A\bar{C}H_{11}$ are still present in both mortars containing metakaolin, but with lower intensity compared to 28 days (Fig. 4B).

Although phenolphthalein test at 180 days (Table 4) shows that all the mortars are fully carbonated, portlandite diffractions are still detected in AL and BAL patterns (Fig. 3C), meaning that the carbonation process reached the mortar core, but some $Ca(OH)_2$ particles remained uncarbonated. $C_4A\bar{C}H_{11}$ disappears at 180 days due to its unstable character. Decomposition or decreasing tendency of $C_4A\bar{C}H_{11}$ with curing time was also observed in author's previous works [18,21].

4.2.2. Mineralogical composition of mortars exhibited to NaCl solution

In coastal areas the mortars might be directly exposed to seawater, which is responsible for ingress of chlorides and subsequent degradation of external renders. An influence of Cl^- on mineralogical composition of mortars after 28, 90 and 180 days of curing was

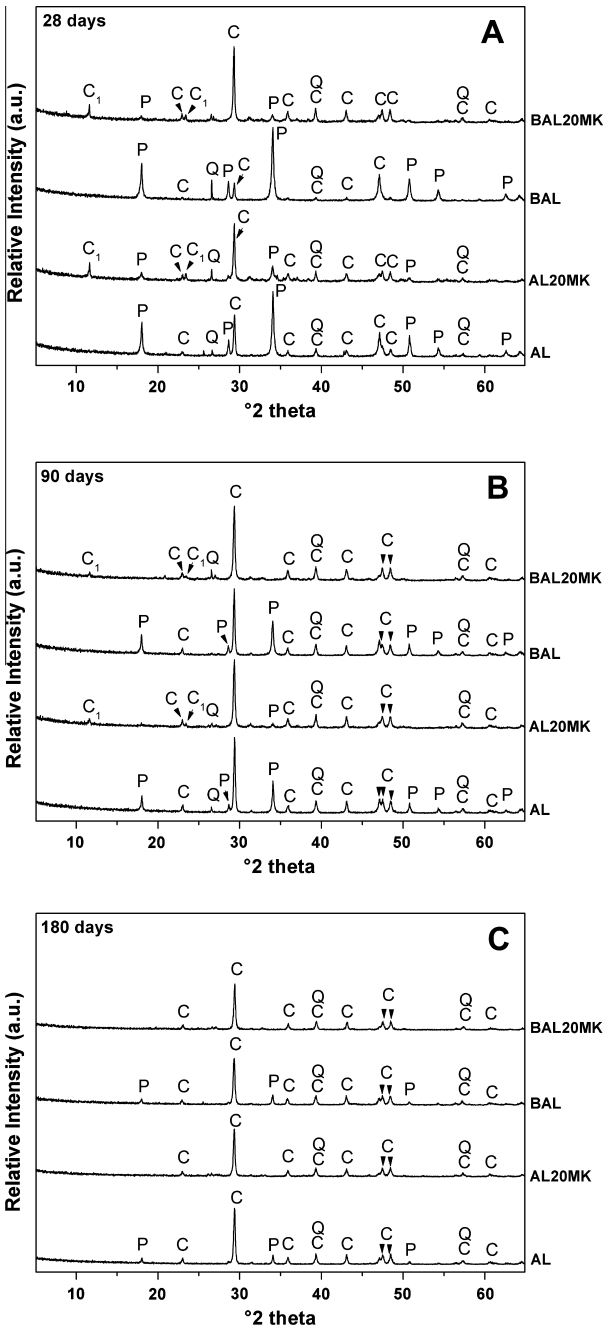

Fig. 4. XRD patterns of non-treated mortars at (A) 28, (B) 90 and (C) 180 days. (C – calcite, C_1 – monocarboaluminate, P – portlandite, Q – quartz).

Table 3
Chemical analysis of materials.

	SiO_2 (%)	Al_2O_3 (%)	Fe_2O_3 (%)	MnO (%)	MgO (%)	CaO (%)	Na_2O (%)	K_2O (%)	TiO_2 (%)	P_2O_5 (%)	LOI* (%)
Sand APAS12	92.86	3.77	0.23	nd**	nd	0.10	nd	3.14	0.02	0.03	0.35
Sand APAS20	95.30	2.51	0.14	nd	nd	0.06	nd	2.24	0.02	0.04	0.29
Sand APAS30	93.17	3.76	0.13	nd	nd	0.03	nd	3.15	0.04	0.05	0.22
Air lime	nd	0.01	0.15	0.01	3.09	76.74	nd	0.02	0.04	0.01	20.45
Metakaolin	54.39	39.36	1.75	0.01	0.14	0.10	nd	1.03	1.55	0.06	1.90
Bentonite	63.00	19.50	2.60	nd	3.90	1.70	0.40	0.90	nd	nd	6.20

* Loss on ignition.
** nd – not detected.

Table 4
Degree of carbonation by phenolphthalein test.

Curing time	Mortar	Degree of carbonation (%)
28 days	AL	36
	BAL	23
	AL20MK	36
	BAL20MK	51
90 days	AL	84
	BAL	80
	AL20MK	91
	BAL20MK	100
180 days	AL	100
	BAL	100
	AL20MK	100
	BAL20MK	100

verified by XRD analysis (Fig. 5A–C). Mortars subjected to salt resistance testing (Fig. 5A–C) contain new mineral phases in comparison with non-treated ones (Fig. 4A–C). At 28 days of curing in mortars with metakaolin (AL20MK and BAL20MK), rather than monocarboaluminate $C_4A\bar{C}H_{11}$ ($3CaO{\cdot}Al_2O_3{\cdot}CaCO_3{\cdot}11H_2O$), the formation of new mineral phases such as Friedel's salt – hydrocalumite ($Ca_4Al_2O_6Cl_2{\cdot}10H_2O$), with characteristic peaks at 11.2°, 22.6° and 31.05° 2θ and sodalite ($K_{7.7}Na_{0.3}(AlSiO_4)_6(ClO_4)_2$) with diffraction at 23.4° 2θ (Fig. 5A) is observed. Halite as a product of NaCl crystallization is identified in all the mortars (27.3°, 31.7° and 45.4° 2θ), as well as portlandite and calcite.

At 90 days of curing, the tested mortars (with BAL exception) seem fully carbonated due to the absence of portlandite and the existence of intense calcite peaks in the mortars patterns. None of pozzolanic products or new minerals formed as a result of Na^+ and Cl^- exchange with pozzolans were found (Fig. 5B). This is also due to the fact that quantity of $C_4A\bar{C}H_{11}$ in non-treated mortars decreases with curing time (Fig. 4B and C) and in the system there was not any mineral phase to react with Na^+ and/or Cl^-, just halite crystals were detected (Fig. 5B). XRD patterns of mortars at 180 days are alike with those at 90 days (Fig. 5C). Calcite diffractions dominate in all the mortars with minor presence of halite.

4.2.3. Microstructure of non-treated mortars

Morphology of AL, BAL, AL20MK and BAL20MK mortars was studied using scanning electron microscopy (Fig. 6A–F). Images were made after 28 days as at this curing time, the mortars show according to XRD the largest differences in mineralogy (Fig. 4A). Fig. 6A illustrates typical structure of carbonated matrix of AL mortar. In Fig. 6B is shown an evidence of pozzolanic activity of BAL mortar, where needles of calcium aluminiumsilicate are formed (Fig. 6E). None of pozzolanic products were detected in XRD analysis of BAL (Fig. 4A–C), meaning that the development of reaction between bentonite and portlandite was carried out at a much poorer level than in case of metakaolin. Rod shaped particles of calcium aluminiumsilicate are also identified in AL20MK mortar (Fig. 6C and F); however in more extend level than in BAL. Microstructure of BAL20MK is very similar with AL20MK mortar, where pozzolanic products are heterogeneously distributed in whole mortar matrix (Fig. 6D).

4.2.4. Microstructure of mortars exhibited to NaCl solution

More detailed impact on microstructure of the mortars after the test of NaCl resistance provide SEM images at 28 days (Fig. 7A–I). Fig. 6A shows halite crystals, which were identified on the surface and also in the inside pores of AL mortar. It was found out that NaCl crystals that fill the pores of BAL are of cubic shape, while those on the surface have a flat form (Fig. 7B and C). Hexagonal crystals of hydrocalumite ($Ca_4Al_2O_6Cl_2{\cdot}10H_2O$) are formed in AL20MK mortar;

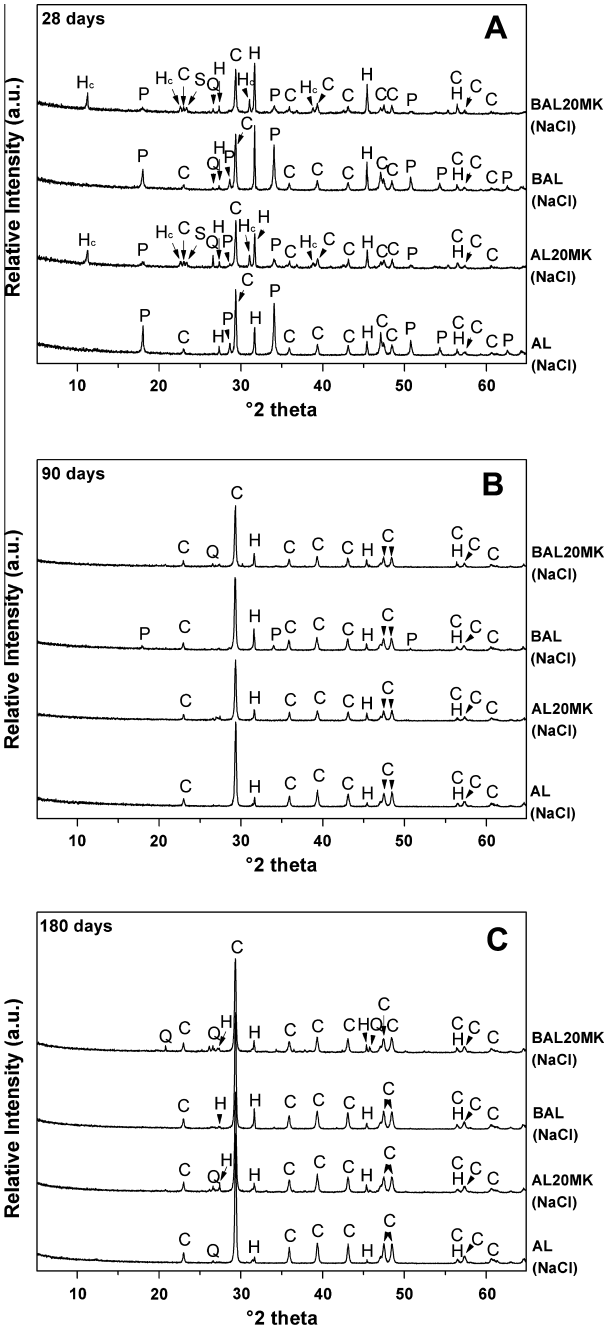

Fig. 5. XRD patterns of mortars exhibited to NaCl solution at (A) 28, (B) 90 and (C) 180 days. (C-calcite, C_1 – monocarboaluminate, H – halite, Hc – hydrocalumite, P – portlandite, Q – quartz, S – sodalite).

also detected in its XRD pattern (Fig. 5A) are illustrated in Fig. 7D and I. Detail on halite crystallization in pore of AL20MK is shown in Fig. 6E. In case of both AL20MK and BAL20MK mortars, there are found pores in which crystallization of halite caused internal tensions associated with the development of cracks (Fig. 7F–H).

4.2.5. Mechanical properties

4.2.5.1. Flexural strength of non-treated mortars. High flexural resistance is one the most important properties of mortars to be applied as renders. Evolution of flexural strength (R_f) values with time of curing is shown in Fig. 8. At 28 days of curing, the differences in the values are not too substantial ranging between 0.16

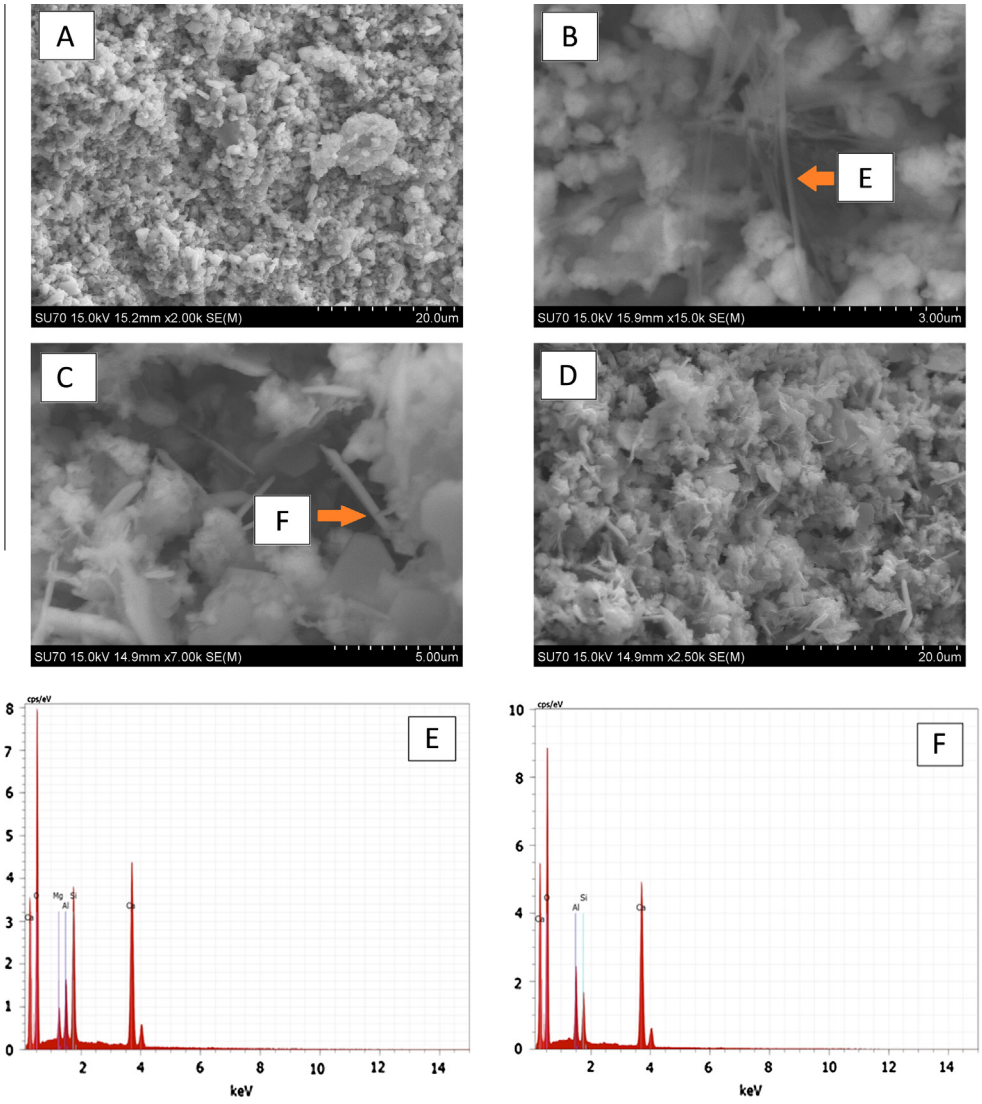

Fig. 6. SEM images of non-treated mortars at 28 days. (A) AL, (B) BAL; (C) AL20MK, (D) BAL20MK, (E) EDS analysis of B, (F) EDS analysis of C.

(BAL20MK) – 0.22 (AL) MPa. This means that substitution of lime by any additive did not enhance R_f at early age. At 90 days, an improvement in flexural resistance is observed in AL and BAL mortars from 0.22 to 0.29 MPa. However it is also noticeable, that bentonite addition in AL mortar did not cause improvement or decrease in flexural strength and AL with BAL reach similar R_f values. On the other hand, AL20MK shows a slight rise in R_f, while no improvement is noticed in BAL20MK mortar. AL and BAL mortars display continuous strength improvement with ageing and, at 180 days, both mortars reach ~0.30 MPa. However, AL20MK and BAL20MK, mortars with MK show a drop in flexural strength, reaching half R_f values compared with those without MK (Fig. 8). AL and BAL mortars show a gradual increase of R_f with curing age due to the fact, that they still contain non reacted portlandite at 180 days, which can carbonate and increase mortaŕs strength even after 180 days (Fig. 4C). Decreasing trend in R_f with curing time of mortars with metakaolin is assigned to the decomposition of non-stable monocarboaluminate $C_4A\bar{C}H_{11}$ as confirmed in XRD patterns of AL20MK and BAL20MK (Fig. 4A–C).

4.2.5.2. Compressive strength of non-treated mortars. Compressive strength (R_c) development of mortars at 28, 90 and 180 days is reported in Fig. 9. The results at 28 days show a much higher variation when compared to the flexural strength ones with values of ~0.21 MPa (for AL and BAL) to ~0.63 MPa (for AL20MK and BAL20MK). It is obvious that metakaolin addition to lime mortars caused remarkable improvement in R_c at early curing age due to its pozzolanic acivity. At 90 days, all the mortars display an increasing trend of R_c, with more evident rise ~about 100% compared to 28 days in AL and BAL mortars. Nevertheless, top R_c values reaches AL20MK with 0.75 MPa followed by BAL20MK with 0.64 MPa. At 180 days, the mortars show similar tendency as in case of their flexural strength (Figs. 8 and 9). Growth of R_c is observed in AL and BAL (25% and 35%, respectively) and decrease in AL20MK and BAL20MK (15% and 7%, respectively) compared to 90 days. As described in previous part, the dropping tendency of metakaolin mortars in their mechanical resistances from 90 to 180 days is related to the lack of portlandite to carbonate, as mortars are already at 90 days fully carbonated (Fig. 4B). Other reason is the disappearance of monocarboaluminate at 180 days (Fig. 4C), what makes mortars more susceptible to fragility. Moreover, even if MK mortars presented very high compressive resistances in early ages of curing, at 180 days AL together with AL20MK mortar reach 0.65 MPa. The lowest compressive strength was during all curing times observed in BAL mortar (0.54 MPa).

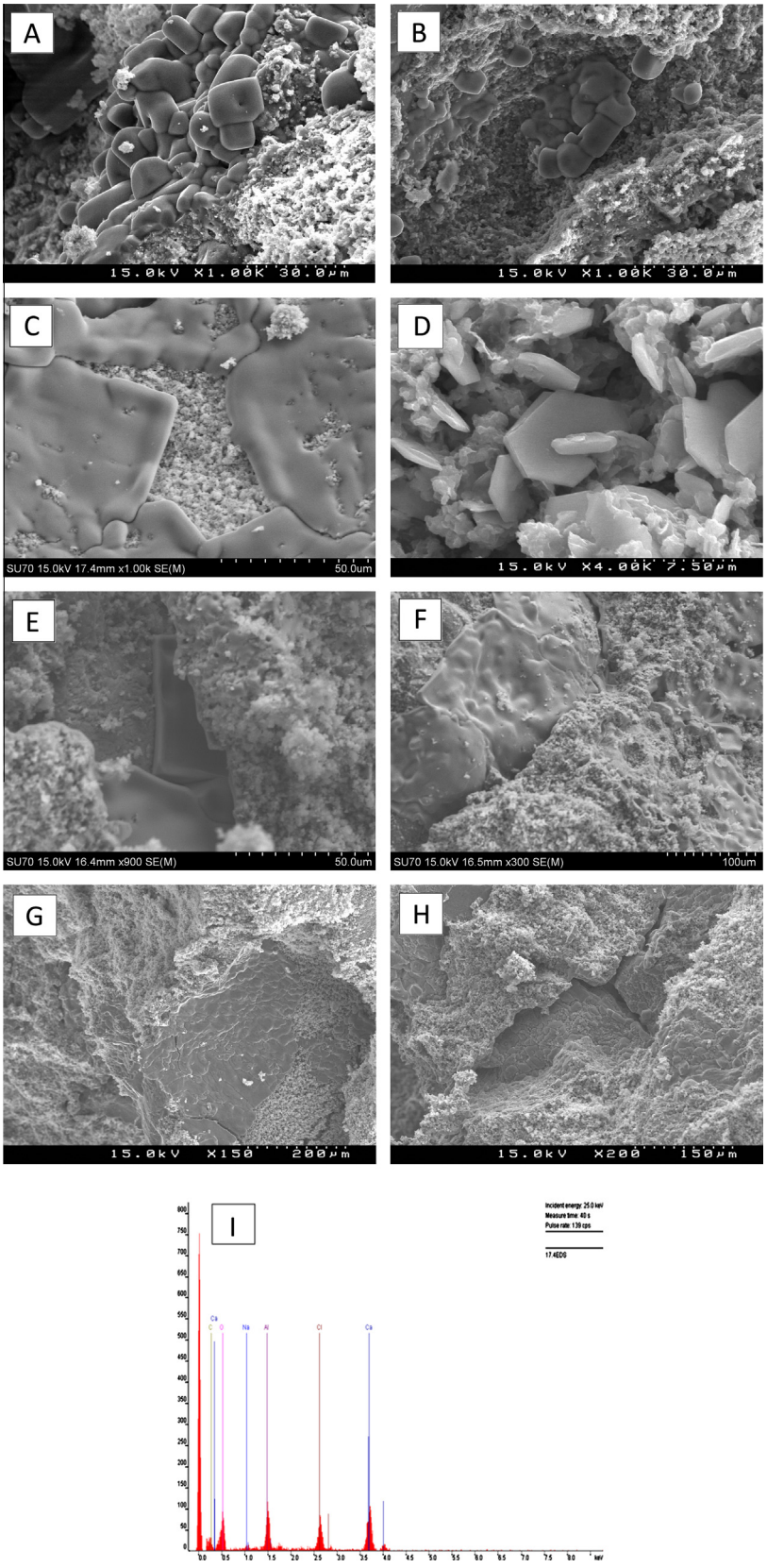

Fig. 7. SEM images of mortars exhibited to NaCl solution at 28 days. (A) AL, (B), BAL (C) BAL; (D) AL20MK; (E) AL20MK; (F) AL20MK, (G) BAL20MK, (H) BAL20MK, (I) EDS analysis of Fig. 7D.

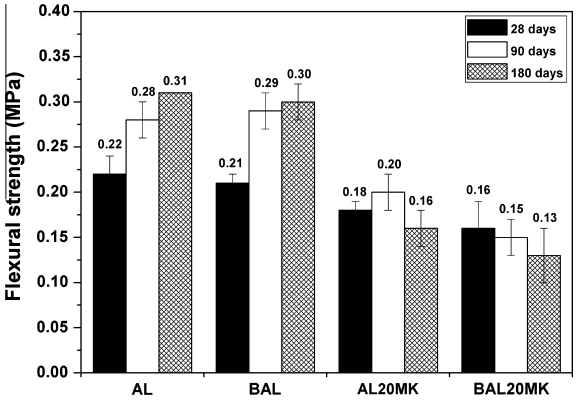

Fig. 8. Flexural strength of non-treated mortars.

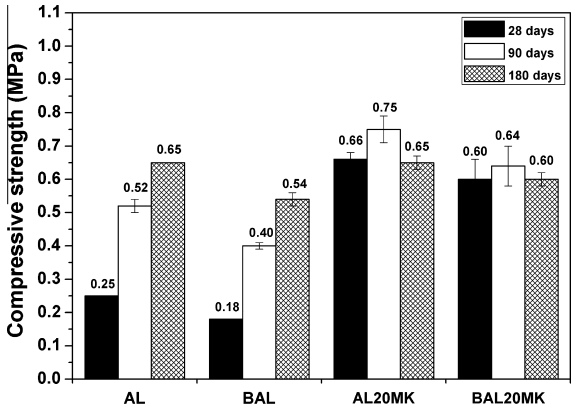

Fig. 9. Compressive strength of non-treated mortars.

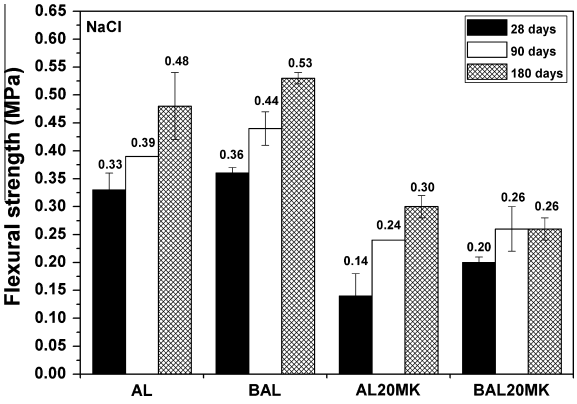

Fig. 10. Flexural strength of mortars exhibited to NaCl solution.

4.2.5.3. Flexural strength of mortars exhibited to NaCl solution. An influence of NaCl on mechanical properties of mortars is reported in Figs. 10 and 11. In case of flexural strength (Fig. 10), mortars demonstrate similar trend as those without treatment (Fig. 8); meaning that mortars with MK (AL20MK and BAL20MK) show decreasing values compared to AL and BAL. Moreover, in comparison with Fig. 8; AL, BAL and BAL20MK mortars show 50%, 71% and 25% rise in R_f, while flexural strength of AL20MK drops from 0.18 to 0.14 MPa. This can be explained by formation of hydrocalumite ($Ca_4Al_2O_6Cl_2{\cdot}10H_2O$) (Fig. 7D) in AL20MK, as its hexagonal crystals produce more porous mortar structure and thus less

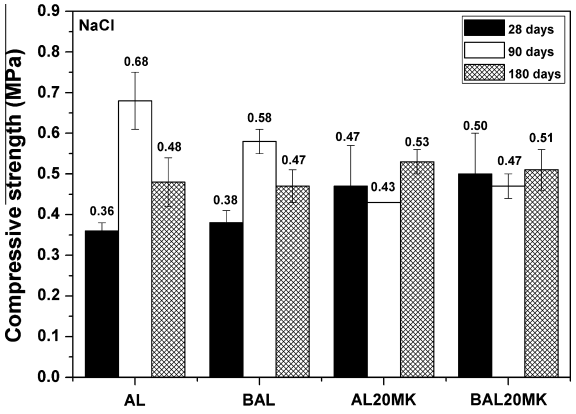

Fig. 11. Compressive strength of mortars exhibited to NaCl solution.

resistant on flexural load. In addition, as it can be seen in Fig. 7E and F, the growth of halite crystals in pores of metakaolin mortars caused internal tensions accompanied with the development of cracks, which are responsible for reduction in flexural strength. At 90 days of curing, flexural strength values of all the mortars increase and are higher compared to non-treated ones. At 180 days, AL (23%), BAL (20%) and AL20MK (25%) show increasing trend, in comparison with their values at 90 days (Fig. 10). BAL20MK mortar stays without any significant change (0.26 MPa). It is important to mention that even after the mortars were exposed to extreme saline environment, all of them reached at 180 days higher R_f than untreated ones (Figs. 8 and 10). Likewise, the best behaviour in term of flexural resistance affirms BAL mortar during all curing times.

4.2.5.4. Compressive strength of mortars exhibited to NaCl solution. The development of compressive strength of mortars exhibited to NaCl solution with ageing shows Fig. 11. R_c values of NaCl mortars at 28 days do not follow the trend of non-threated mortars and the differences in compressive strength of individual mortars are not as substantial as in Fig. 9 at 28 days. Nevertheless, compressive strength of AL and BAL improved about 44 and ~100%, respectively. However, 40% and 20% decrease was observed in AL20MK and BAL20MK mortars, respectively. Even so, AL20MK and BAL20MK provide higher strengths than AL and BAL.

The reason of R_c increase in AL and BAL is, that the mortars without MK have bigger pores than those with MK. Thus the crystallization of NaCl in pores does not create any tensions generating cracks, but on the contrary, crystals fulfilling pores cause more compact, dense and more resistant structure. At 90 days of curing, AL and BAL follow growing tendency of R_c as at 28 days, reaching higher values (0.68 and 0.58 MPa, respectively) compared to AL20MK (0.43 MPa) and BAL20MK (0.47 MPa) (Fig. 11) and also compared to non-threated AL (0.52 MPa) and BAL (0.40 MPa) (Fig. 9). On the other hand, after 180 days, unforeseen behaviour of decrease in R_c show AL (42%) and BAL (23%); and a slight increase exhibit AL20MK (23%) and BAL20MK (9%) mortars (Fig. 11). In the end, all the mortars reach similar compressive resistances ranging between 0.47 (BAL) – 0.53 MPa (AL20MK). These values are lower compared to those of non-treated mortars ranging of 0.54 (BAL) – 0.65 MPa (AL; AL20MK).

4.3. Mortars applied on adobes

4.3.1. Artificial ageing

Gravimetric analysis of all mortars applied on adobes was verified every 7 days during period of 12 weeks, as is reported in

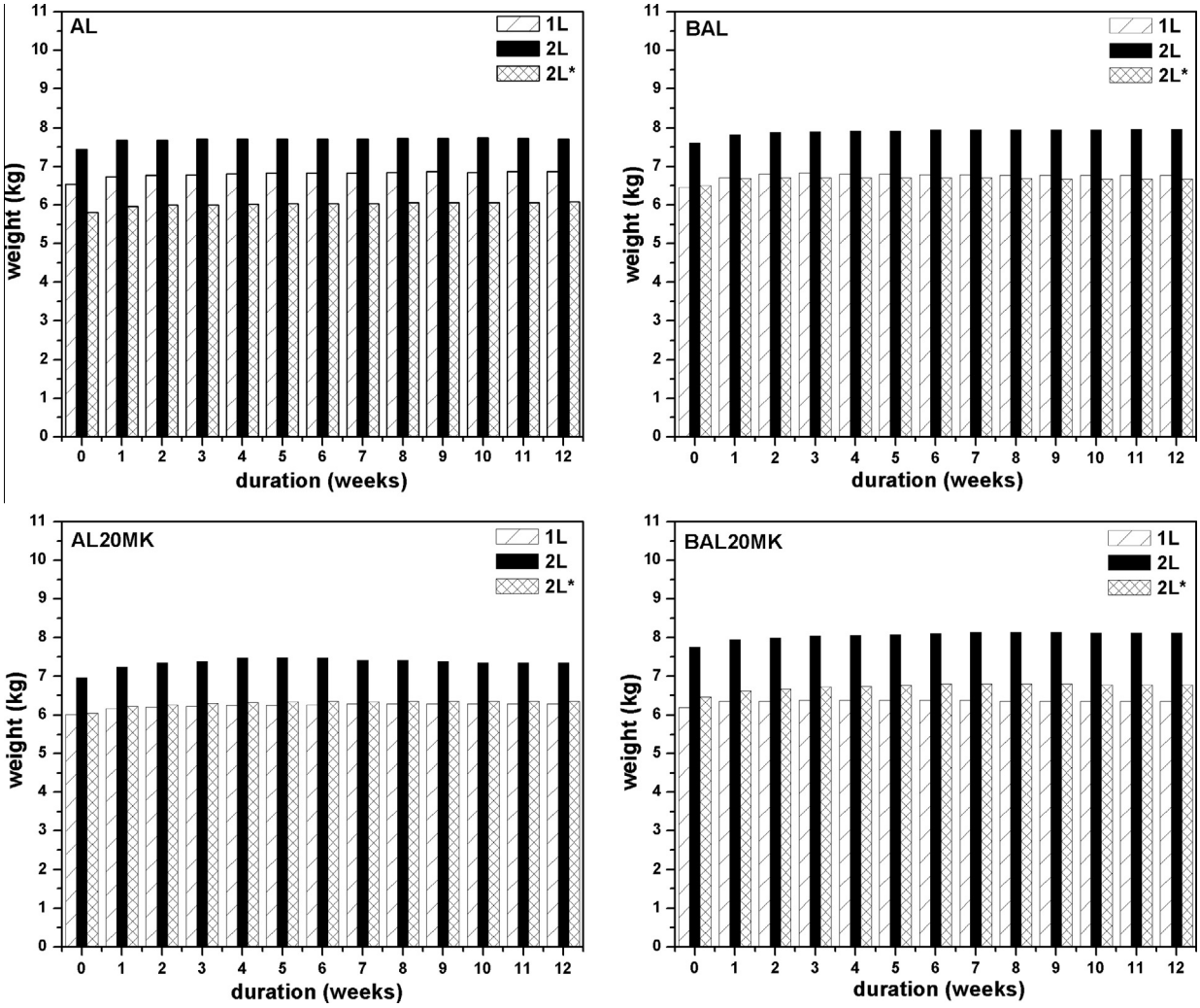

Fig. 12. Gravimetric analysis of mortars during artificial ageing. *1st layer applied as spatterdash.

Fig. 12. It is noticeable that the major mass variations in case of all types of mortars and all types of layers are observed in the first 1–2 weeks. The reason is that the adobes with mortars contained moisture due to the conditions of the chamber, in which they have undergone the curing (65% of RH and 20 °C). But, after the first week of artificial ageing, the adobes were taken from the climatic chamber and always placed in a furnace at 30 °C for 2 h before weighing, to keep the same conditions after every analysing period. Moreover, after the detailed verification of the results, a greater discrepancy combined with loss of weight after the sixth week of cycles was observed in AL20MK mortar applied in two layers (2L) (Fig. 12). The weight loss of AL20MK is a result of its superficial degradation, as is illustrated in Fig. 13. It is evident a clear detachment of top most layer from the rest of the mortar substance, with visible cracks. AL, BAL and BAL20MK mortars do not suffer any visual or mass changes. It is also apparent that in the rest of mortars there are not differences in results comparing individual forms of traditional application (1 layer, 2 layers, 1 layer plus spatterdash) and all seem equally resistant to artificial ageing exposure.

4.4. Mortars applied on adobe wall

4.4.1. Adhesion to background

The strength of mortar's adhesion to the substrate was analysed by pull-off test. The results at 30, 60 and 90 days of curing represents Fig. 14. The final values are low, with the highest discrepancies at 1 month, ranging between 0.018 (AL) – 0.1 (BAL20MK) MPa. It means that BAL20MK mortar shows the best adhesion to adobe substrate at early ages of curing. Moreover, similar values of pull-off were observed in Veiga et al. [47] and Andrejkovičová et al. [18]. After 2 months, adhesion values increase for all mortars with exception of BAL20MK and all the mortars show comparable adhesive strengths 0.055 (AL, BAL), 0.067 (AL20MK) and 0.061 (BAL20MK) MPa. These values stay unchanged after 90 days for AL and BAL mortars. A negligible growth (6%) is observed in AL20MK, while BAL20MK shows a 42% drop with value of 0.043 MPa (Fig. 14). AL20MK mortar displays the best adhesion strength at later curing ages. Regarding to the type of fracture, both: adhesive (fracture at the interface between mortar and adobe substrate) and cohesive type (fracture in the mortar itself) were found. According to the Standard [45], the values obtained in adhesive type of fracture are considered equals to the adhesive strength. This type of fracture was detected predominantly in both mortars with metakaolin and in case of AL at 3 months. On the other hand, preferable cohesive type prevails in AL and BAL mortars and in AL20MK at 30 days. The measured values for cohesive fracture in mortar itself are lower than the real adhesive strength between adobe and mortar (Fig. 14).

4.4.2. Karsten tube penetration test

Ambient water (rain, see, underground) belongs to those impacts from the environment, which negatively influences the

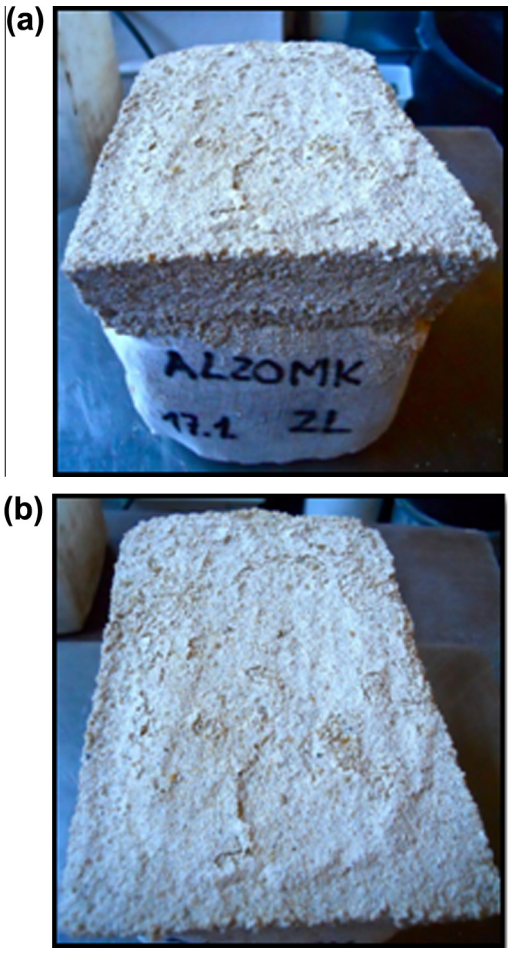

Fig. 13. Degradation of AL20MK mortar's surface appeared after 6 weeks of artificial ageing.

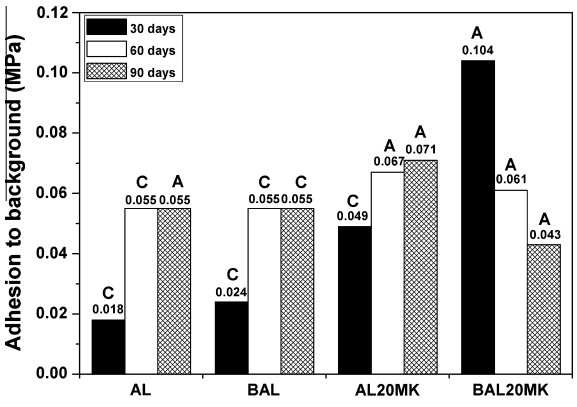

Fig. 14. Pull-off test of mortars. (A-adhesive, C-cohesive type of fracture).

stability of renders by creation of cracks by wetting and drying processes, or by efflorescence soluble salts. It is well-known that the renders should be characterised by low water absorption ([48] Groot, 2010); while water vapour permeability should be as high as possible [3]. Karsten tube test was used to measure the penetration of a given amount of water (4 ml) in time (Fig. 15). Table 5 reports the results of Karsten tube test of mortars applied on the adobe wall. Comparing the values at 30 days, the slowest water absorption is observed by BAL20MK with 325 s at 4 ml, while the fastest is manifested by AL (53 s at 4 ml). After 60 days

Fig. 15. Demonstration of Karsten tube testing on mortar.

Table 5
Karsten tube values of mortars applied on adobe wall.

Karsten tube (ml)	Time of absorption (s)			
	AL	BAL	AL20MK	BAL20MK
30 days				
1	6	12	19	29
2	16	29	50	100
3	32	50	96	203
4	53	77	162	325
60 days				
1	4	5	8	14
2	11	13	24	48
3	20	26	48	105
4	35	45	85	180
90 days				
1	5	11	15	30
2	12	28	47	77
3	22	51	100	142
4	34	82	180	222

a slight drop in values is detected for all the mortars, meaning that they absorb water faster compared to 30 days (Table 5). This is related to microstructural changes and pores creation during curing. Nevertheless, BAL20MK mortar shows the best behaviour (180 s at 4 ml) followed by AL20MK (85 s), BAL (45 s) and then AL (35 s) at 4 ml. With time of curing, Karsten tube values show a rise, compared to 90 days, keeping the trend of previous curing ages. The slowest water absorption shows BAL20MK (222 s), continuing by faster AL20MK (180 s) and BAL (82 s) mortars. AL mortar provides the worst performance related to water penetration with 34 s at 4 ml. This means that BAL20MK mortar has the best microstructure; avoiding rapid water intake into the mortar matrix.

4.4.3. Summary of all the tests performed on the mortars

Table 6 provides summary of all the tests carried out on the mortars. It is obvious that BAL mortar shows the best performance

Table 6
Final evaluation of testing.

Test	AL	BAL	AL20MK	BAL20MK
Lower degree of carbonation		✗		
Higher flexural strength	✗	✗		
Higher flexural strength after NaCl treatment		✗		
Resistance to artificial ageing	✗	✗		✗
Adhesion to background			✗	
Karsten tube test				✗

in most experiments. Even in case of adhesion to background and Karsten tube test, BAL mortar shows equal or better results compared to AL, respectively. This means that just 5 wt.% of lime substitution by natural bentonite, provides the mortar mixture with the best characteristics to be used as render of historical adobe buildings.

5. Conclusions

Four different types of mortars based on lime (AL) with addition of bentonite (BAL), metakaolin (AL20MK) and bentonite and metakaolin (BAL20MK) were analysed in terms of utilization as repair mortars for historical adobe buildings. The main results can be summarized as follows:

(a) Metakaolin shows pozzolanic activity by creation of monocarboaluminate $C_4A\overline{C}H_{11}$ confirmed by XRD analysis.
(b) No pozzolanic activity of bentonite is proved by XRD analysis, but is revealed by SEM analysis by formation of rod shaped particles of calcium aluminiumsilicate.
(c) Decomposition of monocarboaluminate in AL20MK and BAL20MK is responsible for low flexural strength of metakaolin mortars.
(d) Bentonite decelerates the carbonation process of AL mortar in early ages of curing enabling a continuous hardening of mortar without cracks formation.
(e) Friedel salt hydrocalumite ($Ca_4Al_2O_6Cl_2{\cdot}10H_2O$) and sodalite ($K_{7.7}Na_{0.3}(AlSiO_4)_6(ClO_4)_2$) are the new products identified in mortars containing metakaolin during the test of NaCl resistance at 28 days.
(f) SEM analysis confirms that crystallization of halite in mortars with metakaolin is accompanied with internal tensions and crack development. This is responsible for lower flexural resistances of metakaolin mortars compared to AL and BAL.
(g) All mortars show, regardless the type of layering, very high resistance for extreme weather conditions during artificial ageing. The only exception is AL20MK mortar applied in 2 layers, where superficial degradation is observed after 6 weeks of testing.
(h) Both types of fractures adhesive (between mortar and adobe substrate) prevailing in mortars with metakaolin and cohesive (in mortar itself) prevailing in mortars without metakaolin, are found. The best adhesion strength displays AL20MK mortar at later ages.
(i) The ideal microstructure providing low water penetration abilities by Karsten tube test shows BAL20MK mortar during all testing periods.
(j) Based on all the tests performed on the mortars, 5 wt.% of lime substitution by natural clay – bentonite provides the mortar mixture with the best characteristics to be used as render of historical adobe buildings.

Acknowledgements

This research was supported by PEst-C/CTE/UI4035/2011 and COMPETE Programme PEst-OE/CTE/UI4035/2014. The authors are grateful to Envigeo a.s., Banská Bystrica, Slovakia for providing the bentonite used in this study.

References

[1] Costa CS, Rocha F, Varum H, Velosa A. Influence of the mineralogical composition on the properties of adobe blocks from Aveiro, Portugal. Clay Miner 2013;48:749–58.
[2] Silveira D, Varum H, Costa A, Martins T, Pereira H, Almeida J. Mechanical properties of adobe bricks in ancient constructions. Constr Build Mater 2012;28:36–44.
[3] Barbero-Barrera MdM, Maldonado-Ramosa L, Van Balen K, García-Santosa A, Neila-González FJ. Lime render layers: An overview of their properties. Int J Archit Herit 2014;14:326–30.
[4] Coroado J, Paiva H, Velosa A, Ferreira VM. Characterization of renders, joint mortars and adobes from traditional constructions in Aveiro-(Portugal). Int J Archit Herit 2010;4:102–14.
[5] Schueremans L, Cizer Ö, Janssens E, Serré G, Van Balen K. Characterization of repair mortars for the assessment of their compatibility in restoration projects: research and practice. Constr Build Mater 2011;25(12):4338–50.
[6] Aggelakopoulou E, Bakolas A, Moropoulou A. Properties of lime–metakolin mortars for the restoration of historic masonries. Appl Clay Sci 2011;53:15–9.
[7] Arıoglu N, Acun SA. A research about a method for restoration of traditional lime mortars and plasters: a staging system approach. Build Environ 2006;41:1223–30.
[8] Moropoulou A, Bakolas A, Moundoulas P, Aggelakopoulou E, Anagnostopoulou S. Strength development and lime reaction in mortars for repairing historic masonries. Cem Concr Compos 2005;27:289–94.
[9] Arizzi A, Viles H, Cultrone G. Experimental testing of the durability of lime-based mortars used for rendering historic buildings. Constr Build Mater 2012;28:807–18.
[10] Arizzi A, Cultrone G. Aerial lime based-mortars blended with a pozzolanic additive and different admixtures: a mineralogical, textural and physical-mechanical study. Constr Build Mater 2012;31:135–43.
[11] Faria P, Henriques F, Rato V. Comparative evaluation of lime mortars for architectural conservation. J Cult Herit 2008;9:338–46.
[12] Lanas J, Sirera R, Alvarez JI. Study of the mechanical behavior of masonry repair lime-based mortars cured and exposed under different conditions. Cem Concr Res 2006;36:961–70.
[13] Vejmelková E, Keppert M, Keršner Z, Rovnaníková P, Černý R. Mechanical, fracture-mechanical, hydric, thermal, and durability properties of lime–metakaolin plasters for renovation of historical buildings. Constr Build Mater 2012;31:22–8.
[14] Velosa AL, Rocha F, Veiga R. Influence of chemical and mineralogical composition of metakaolin on mortar characteristics. Acta Geodyn Geomater 2009;153:1–6.
[15] Sabir BB, Wild S, Bai J. Metakaolin and calcined clays as pozzolans for concrete: a review. Cem Concr Comp 2001;23:441–54.
[16] Siddique R, Klaus J. Influence of metakaolin on the properties of mortar and concrete: a review. Appl Clay Sci 2009;43:392–400.
[17] Andrejkovičová S, Ferraz E, Velosa AL, Silva AS, Rocha F. Fine sepiolite addition to air lime metakaolin mortars. Clay Miner 2011;46:621–35.
[18] Andrejkovičová S, Velosa AL, Rocha F. Air lime–metakaolin–sepiolite mortars for earth based walls. Constr Build Mater 2013;44:133–41.
[19] Martínez-Ramírez S, Puertas F, Blanco-Varela MT. Carbonation process and properties of a new lime mortar with added sepiolite. Cem Concr Res 1995;25:39–50.
[20] Martínez-Ramírez S, Puertas F, Blanco-Varela MT, Thompson GE. Effect of dry deposition of pollutants on the degradation of lime mortars with sepiolite. Cem Concr Res 1998;28:125–33.
[21] Andrejkovičová S, Velosa AL, Gameiro A, Ferraz E, Rocha F. Palygorskite as an admixture to air lime-metakaolin mortars for restoration purposes. Appl Clay Sci 2013;83–84:368–74.
[22] Andrejkovičová S, Ferraz E, Velosa AL, Silva AS, Rocha F. Air lime mortars with incorporation of sepiolite and synthetic zeolite pellets. Acta Geodyn Geomater 2012;9:79–91.
[23] Ferraz E, Andrejkovičová S, Velosa AL, Silva AS, Rocha F. Incorporation of synthetic zeolite pellets in lime-metakaolin mortars. Constr Build Mater 2014;69:243–52.
[24] Andrejkovičová S, Velosa AL, Ferraz E, Rocha F. Influence of clay minerals addition on mechanical properties of air lime-metakaolin mortars. Constr Build Mater 2013;65:132–9.
[25] Ahmad S, Barbhuiya SA, Elahi A, Iqbal J. Effect of Pakistani bentonite on properties of mortar and concrete. Clay Miner 2011;46:85–92.
[26] Memon SA, Arsalan R, Khan S, Lo TY. Utilization of Pakistani bentonite as partial replacement of cement in concrete. Constr Build Mater 2012;30:237–42.

[27] Mirza J, Riaz M, Naseer A, Rehman F, Khan AN, Ali Q. Pakistani bentonite in mortars and concrete as low cost construction material. Appl Clay Sci 2009;45:220–6.
[28] Andrejkovičová S, Rocha F, Janotka I, Komadel P. An investigation into the use of blends of two bentonites for geosynthetic clay liners. Geotext Geomembranes 2008;26:436–45.
[29] Janotka I, Kišš Š, Baslik R. Geosynthetic mat tatrabent-development, production and application. Appl Clay Sci 2002;21:21–31.
[30] Andrejkovičová S, Pentrák M, Jankovič Ľ, Komadel P. Sorption of heavy metal cations on rhyolitic and andesitic bentonites from central Slovakia. Geol Carpath 2010;61:163–71.
[31] Brtáňová A, Melichová Z, Komadel P. Sorption of Cu2+ from aqueous solution by Slovak bentonites. Ceram Silik 2012;56(1):55–60.
[32] Galamboš M, Kufčáková J, Rosskopfová O, Rajec P. Adsorption of cesium and strontium on natrified bentonites. J Radioanal Nucl Chem 2010;283(3):803–13.
[33] Galamboš M, Paučová V, Kufčáková J, Rosskopfová O, Rajec P, Adamcová R. Cesium sorption on bentonites and montmorillonite K10. J Radioanal Nucl Chem 2010;284(1):55–64.
[34] Galamboš M, Rosskopfová O, Kufčáková J, Rajec P. Utilization of Slovak bentonites in deposition of high-level radioactive waste and spent nuclear fuel. J Radioanal Nucl Chem 2011;288(3):765–77.
[35] Galamboš M, Šeršeň F, Rajec P, Daňo M, Kufčáková J, Rosskopfová O, et al. Effect of gamma-irradiation on adsorption properties of Slovak bentonites. J Radioanal Nucl Chem 2012;291(2):481–92.
[36] Galamboš M, Osacký M, Rosskopfová O, Krajňák A, Rajec P. Comparative study of strontium adsorption on dioctahedral and trioctahedral smectites. J Radioanal Nucl Chem 2012;293:889–97.
[37] Galamboš M, Krajňák A, Rosskopfová O, Viglašová E, Adamcová R, Rajec P. Adsorption equilibrium and kinetic studies of strontium on Mg-bentonite, Fe-bentonite and illite/smectite. J Radioanal Nucl Chem 2013;298(2):1031–40.
[38] Alvarez I, Gomez-Gesteira MM, de Castro M, Carvalho D. Comparison of different wind products and buoy wind data with seasonality and interannual climate variability in the southern Bay of Biscay (2000–2009). Deep-sea Res PT II 2014;106:38–48.
[39] Carvalho D, Rocha A, Gómez-Gesteira M. Ocean surface wind simulation forced by different reanalyses: comparison with observed data along the Iberian Peninsula coast. Ocean Model 2012;56:31–42.
[40] Carvalho D, Rocha A, Gómez-Gesteira M, Alvarez I, Silva Santos C. Comparison between CCMP, QuikSCAT and buoy winds along the Iberian Peninsula coast. Rem Sens Environ 2013;137:173–83.
[41] EN 1015-2. Methods of test for mortar for masonry Part 2: Bulk sampling of mortars and preparation of test mortars; 1998.
[42] EN 1015-11. Methods of test for mortar for masonry – Part 11: Determination of flexural and compressive strength of hardened mortar; 1999.
[43] Teutonico JM. A laboratory manual for architectural conservators. Rome: ICCROM; 1988.
[44] EN 1015-18. Methods of test for mortar for masonry – Part 18: Determination of water absorption coefficient due to capillary action of hardened rendering mortar. European Committee of Standardization, Brussels; 2002.
[45] EN 1015-12. Methods of test for mortar for masonry. Determination of adhesive strength of hardened rendering and plastering mortars on substrates; 2000.
[46] Magalhães AC, Veiga MR. Ensaios "in situ" sobre revestimentos de paredes para edifícios antigos. Ensaios preliminares com tubos de Carsten. Lisboa: LNEC, Setembro de 2002. Relatório no. 238/02–NCCt; 2002 [in Portuguese].
[47] Veiga MR, Velosa AL, Magalhães AC. Experimental applications of mortars with pozzolanic additions: characterization and performance evaluation. Constr Build Mater 2009;23:318–27.
[48] Groot C. Performance and repair requirements for renders and plasters. RILEM TC203-RHM, ITAM, Prague; 2010.